doi:10.1038/nature12614

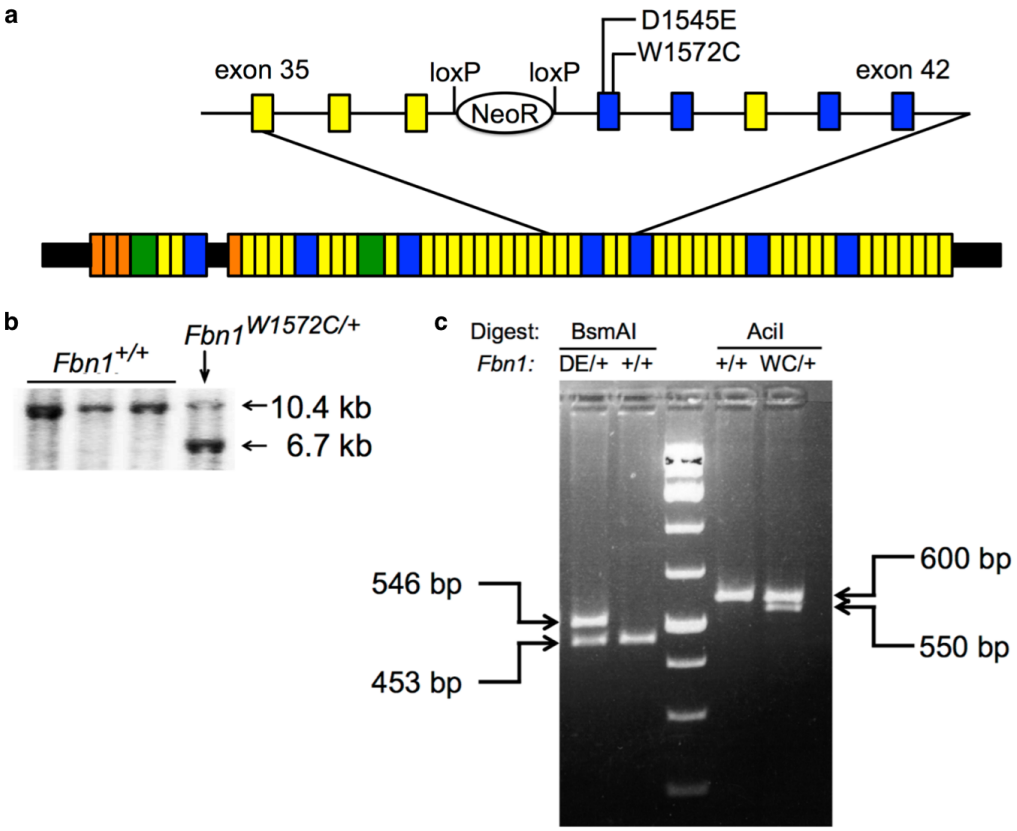

Supplementary Figure S1 | Generation of *Fbn1*$^{D1545E/+}$ and *Fbn1*$^{W1572C/+}$ mice. **a**, Schematic of constructs used to generate *Fbn1*$^{D1545E/+}$ and *Fbn1*$^{W1572C/+}$ mice by homologous recombination. The construct contained a neomycin resistance cassette (NeoR), flanked by loxP sites, that was later removed via breeding to mice expressing Cre-recombinase. **b**, Representative Southern blot (for mutation W1572C) showing proper targeting in embryonic stem (ES) cells prior to blastocyst injection and implantation into pseudopregnant mice. **c,** Mice were genotyped on the basis of creation of a new AciI site (W1572C) or destruction of a BsmAI site (D1545E) in correctly targeted mice. *Fbn1* genotypes: WC/+, *Fbn1*$^{DW1572C/+}$; DE/+, (*Fbn1*$^{D1545E/+}$).

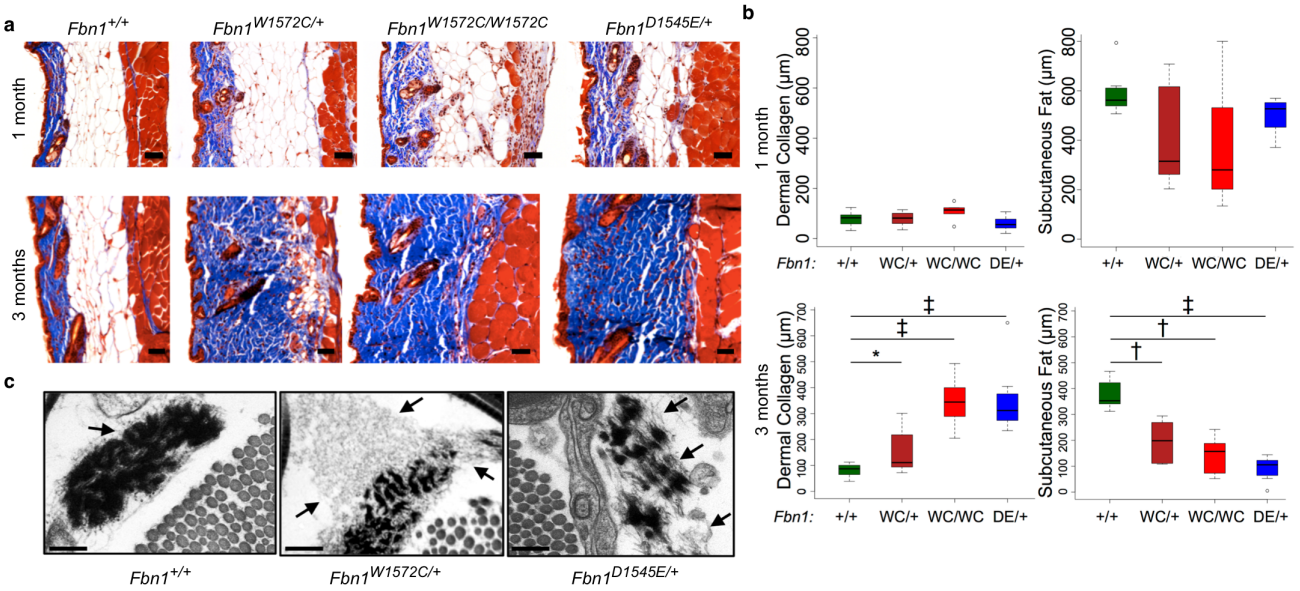

Supplementary Figure S2 | SSS mice show skin fibrosis and dermal accumulation of microfibrillar aggregates. a, Masson's trichrome staining of back skin sections from mutant (genotypes indicated) female mice at 1 month (top panels) and 3 months (bottom panels) of age demonstrates progressive loss of subcutaneous fat and an expanded zone of dense dermal collagen. **b,** Quantification of the thickness of the zones of dermal collagen a nd subcutaneous fat in wild-type and mutant female mice at 1 (top panels) and 3 (bottom panels) months of age. 1 month females: n = 8 (+/+), 8 (WC/+), 8 (WC/WC), 9 (DE/+); 3 month females: n = 12 (+/+), 10 (WC/+), 9 (WC/WC), 9 (DE/+). Scale bars, 50 µm. * $p<0.05$, ** $p<0.01$, † $p<0.001$, ‡ $p<0.0001$. **c,** Electron microscopy shows excessive microfibrillar deposits (black arrows) and sparsely distributed electron-dense (black) elastin in mutant skin. Scale bars, 500 nm.

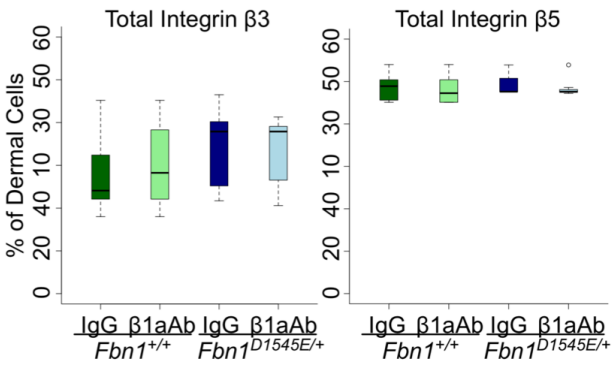

Supplementary Figure S3 | Flow cytometry analysis shows no significant differences in cell-surface expression of total αvβ3 or αvβ5 between SSS mice and wild-type littermates. This did not change with β1aAb treatment. Isotype control-treated: n = 12 (*Fbn1*$^{+/+}$), 9 (*Fbn1*$^{D1545E/+}$), 8 (*Fbn1*$^{W1572C/+}$); β1aAb-treated: n = 12 (*Fbn1*$^{+/+}$), 10 (*Fbn1*$^{D1545E/+}$), 10 (*Fbn1*$^{W1572C/+}$).

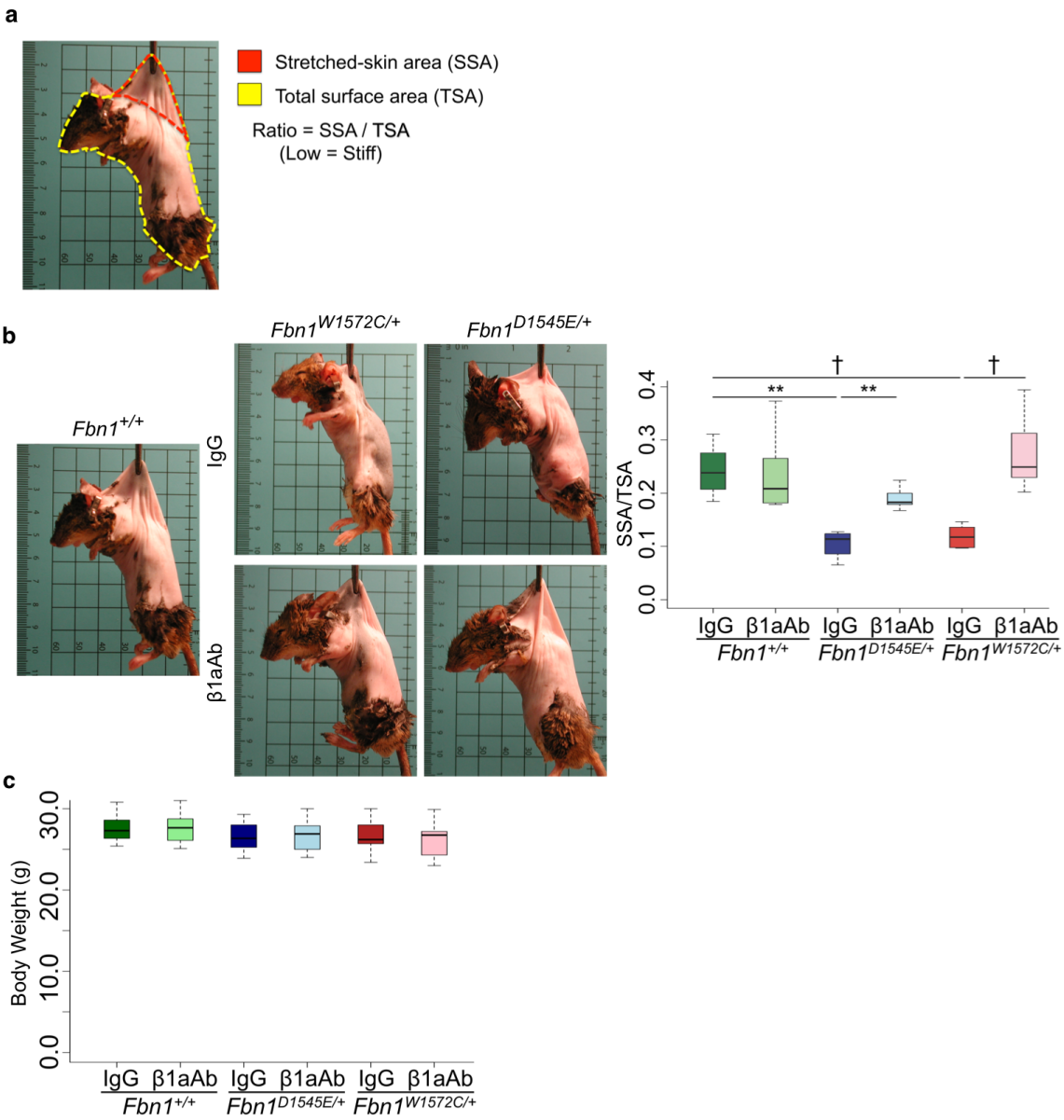

Supplementary Figure S4 | β1 integrin antibody treatment prevents skin fibrosis. a, Schematic showing how the stretched skin area/total surface area (SSA/TSA) ratios were measured. Mice were anesthetized and their back-hair removed. Mice were then briefly suspended by their back skin and photographed in profile in a uniform manner. **b,** Mutant mice showed a reduced SSA/TSA ratio that was normalized upon treatment with β1aAb but not by an isotype-matched control (IgG). **c,** There were no differences in body weight between all experimental groups. Isotype control-treated: n = 12 (*Fbn1*$^{+/+}$), 9 (*Fbn1*$^{D1545E/+}$), 8 (*Fbn1*$^{W1572C/+}$); β1aAb-treated: n = 12 (*Fbn1*$^{+/+}$), 10 (*Fbn1*$^{D1545E/+}$), 10 (*Fbn1*$^{W1572C/+}$). Measurements were performed with NIH image J software (National Institute of Health, Bethesda, MD, USA). * p<0.05, ** p<0.01, † p<0.001, ‡ p<0.0001.

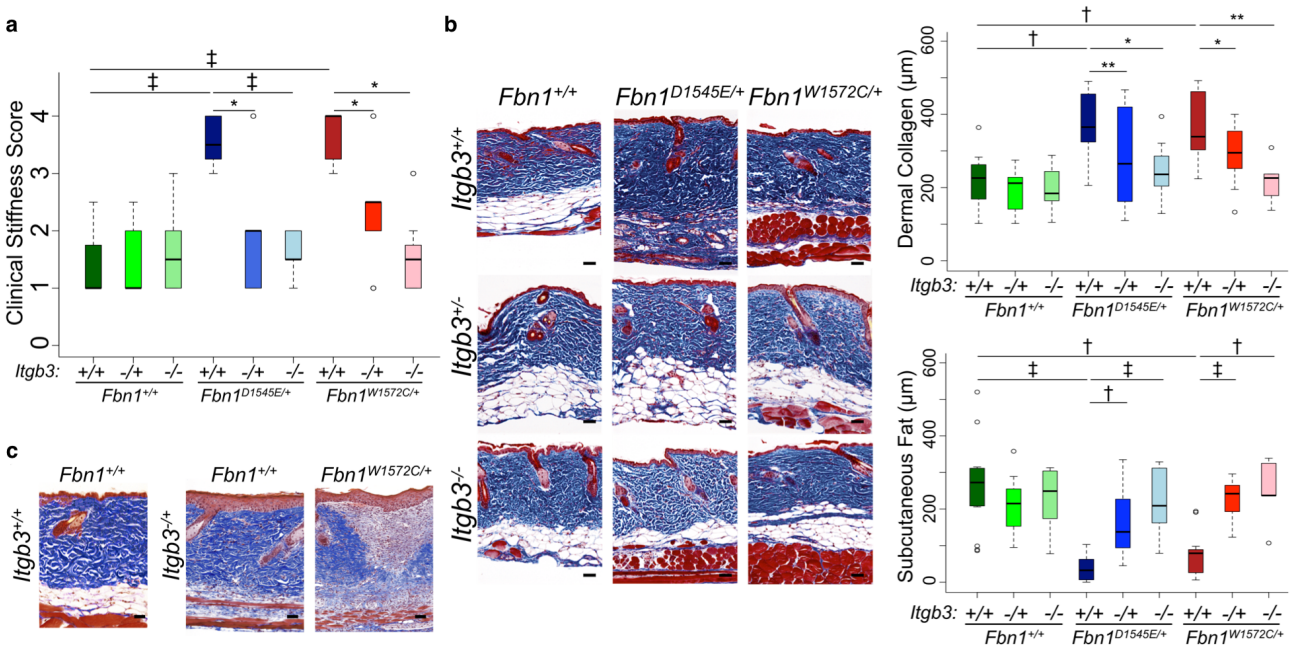

Supplementary Figure S5 | Genetic targeting of integrin β3 prevents skin fibrosis. a, Introduction of haploinsufficiency (-/+) or the null state (-/-) for the gene encoding integrin β3 (*Itgb3*) attenuates or prevents skin stiffening, respectively, in mouse models of SSS. **b,** Histologic and morphometric analyses using Masson's trichrome stain. **c,** A small subset of mice (~12% overall) that are haploinsufficient (-/+) or null (-/-) for *Itgb3*, the gene encoding integrin β3, show focal epidermal hyperplasia and increased cellularity and collagen in the dermis at five months of age. These findings were observed irrespective of *Fbn1* genotype. Scale bars, 50 µm. n = 12 (*Fbn1*$^{+/+}$ and *Itgb3*$^{+/+}$), 13 (*Fbn1*$^{+/+}$ and *Itgb3*$^{-/+}$), 7 (*Fbn1*$^{+/+}$ and *Itgb3*$^{-/-}$), 8 (*Fbn1*$^{D1545E/+}$ and *Itgb3*$^{+/+}$), 18 (*Fbn1*$^{D1545E/+}$ and *Itgb3*$^{-/+}$), 14 (*Fbn1*$^{D1545E/+}$ and *Itgb3*$^{-/-}$), 7 (*Fbn1*$^{W1572C/+}$ and *Itgb3*$^{+/+}$), 9 (*Fbn1*$^{W1572C/+}$ and *Itgb3*$^{-/+}$), 6 (*Fbn1*$^{W1572C/+}$ and *Itgb3*$^{-/-}$). Scale bars, 50 µc. * p<0.05, ** p<0.01, † p<0.001, ‡ p<0.0001.

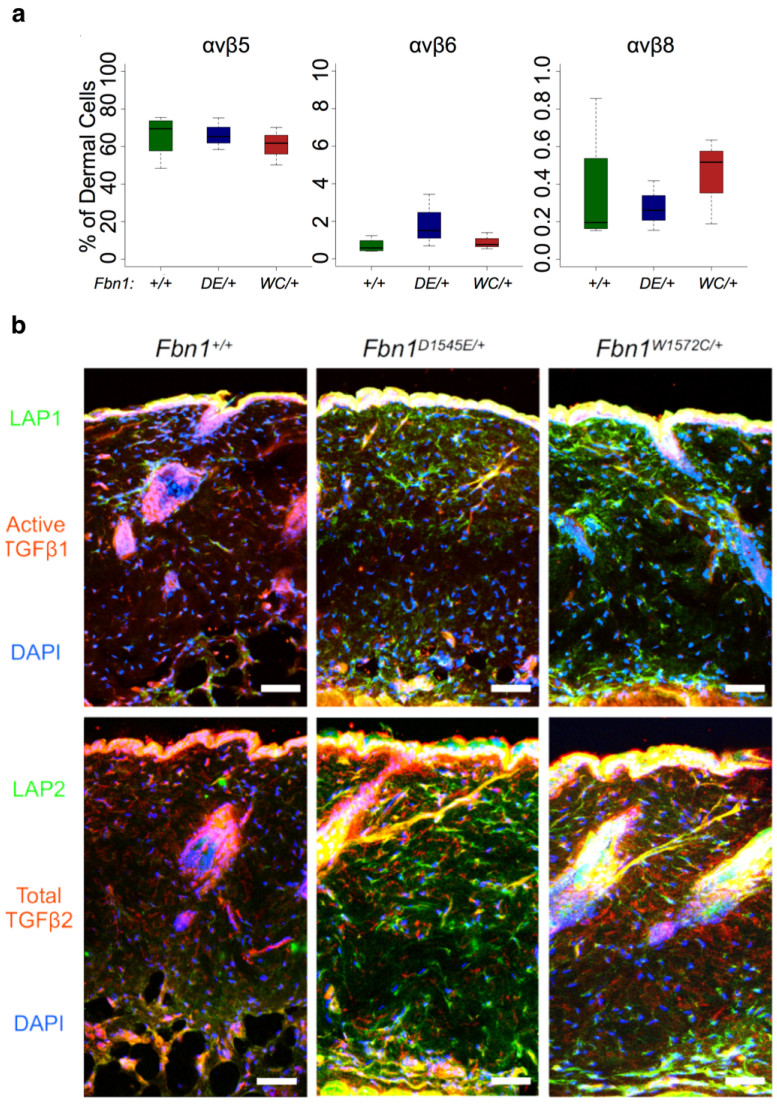

Supplementary Figure S6 | SSS mice show no significant difference in the expression of integrins known to potently support the activation of TGFβ. a, Flow cytometry analysis did not reveal an increase in the expression of integrins known to potently support the activation of TGFβ (αvβ5, αvβ6 or αvβ8) in the dermis of mutant mice, when compared to wild-type littermates. **b,** Immunofluorescence analysis reveals increased latency-associated peptide (LAP)-1, LAP-2 and total TGFβ2 in the dermis of mutant mice, when compared to wild-type littermates. No difference in active (free) TGFβ1 was observed. n = 5 (*Fbn1*$^{+/+}$, +/+), 4 (*Fbn1*$^{D1545E/+}$, DE/+), 4 (*Fbn1*$^{DW1572C/+}$, WC/+). Scale bars, 50 μm.

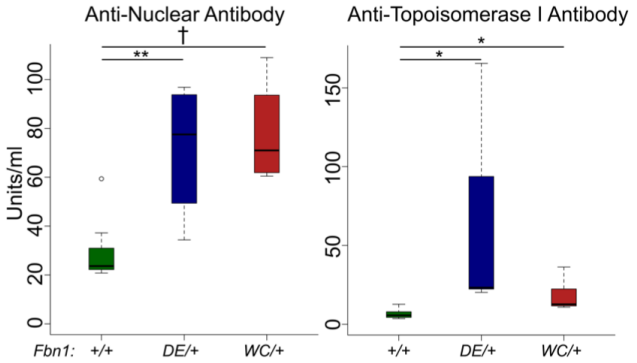

Supplementary Figure S7 | Increased circulating levels of anti-nuclear and anti-topoisomerase I antibodies by enzyme-linked immunosorbent assay (ELISA) in mutant mice at 18 months of age. n = 5 (*Fbn1*$^{+/+}$, +/+), 4 (*Fbn1*$^{D1545E/+}$, DE/+), 4 (*Fbn1*$^{DW1572C/+}$, WC/+). * p<0.05, ** p<0.01, † p<0.001, ‡ p<0.0001.

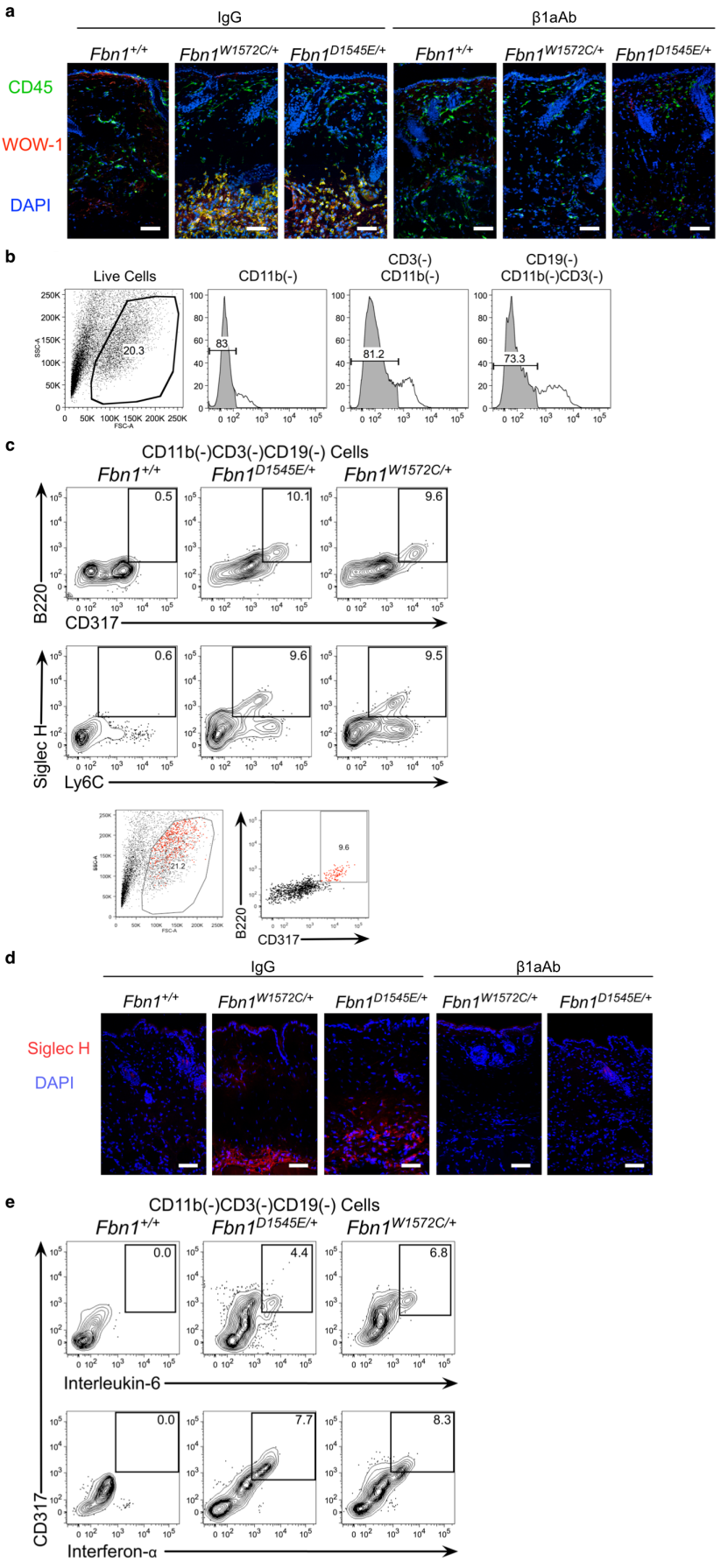
a
IgG
β1aAb
Fbn1+/+
Fbn1W1572C/+
Fbn1D1545E/+
CD45
WOW-1
DAPI
b
Live Cells
CD11b(-)
CD3(-) CD11b(-)
CD19(-) CD11b(-)CD3(-)
20.3
83
81.2
73.3
c
CD11b(-)CD3(-)CD19(-) Cells
0.5
10.1
9.6
B220
CD317
0.6
9.6
9.5
Siglec H
Ly6C
21.2
9.6
d
IgG
β1aAb
Siglec H
DAPI
e
CD11b(-)CD3(-)CD19(-) Cells
0.0
4.4
6.8
Interleukin-6
0.0
7.7
8.3
CD317
Interferon-α

Supplementary Figure S8 | SSS mice show dermal accumulation of plasmacytoid dendritic cells (pDCs). a, Increased deep dermal expression of active integrin β3 in the mutant skin colocalizes with CD45(+) cells derived from the bone marrow; both signals were normalized upon treatment with β1aAb but not with an isotype-matched control (IgG). Isotype control-treated: n = 5 (*Fbn1*$^{+/+}$), 7 (*Fbn1*$^{D1545E/+}$); β1aAb-treated: n = 4 (*Fbn1*$^{+/+}$), 7 (*Fbn1*$^{D1545E/+}$). For panel E: n = 5 (*Fbn1*$^{+/+}$), 4 (*Fbn1*$^{D1545E/+}$), 4 (*Fbn1*$^{DW1572C/+}$). * p<0.05, ** p<0.01, † p<0.001, ‡ p<0.0001. **b,** Gating strategy for pDC identification: First, live cells are gated. Next, CD11b(+) leukocytes, CD3(+) T cells, and CD19(+) B cells are excluded. **c,** Representative flow cytometry plots showing that the cells under consideration are B220+, CD317(high), Siglec H(+), Ly6C(high) and show a conventional size distribution for pDCs. **d,** Immunofluorescent staining confirming the presence of Siglec H(+) cells in the dermis of placebo-treated SSS mice, but absent in that of of wild-type or treated animals. Scale bars, 50 μm. Isotype control-treated: n = 5 (*Fbn1*$^{+/+}$), 7 (*Fbn1*$^{D1545E/+}$); β1aAb-treated: n = 4 (*Fbn1*$^{+/+}$), 7 (*Fbn1*$^{D1545E/+}$). For panel E: n = 5 (*Fbn1*$^{+/+}$), 4 (*Fbn1*$^{D1545E/+}$), 4 (*Fbn1*$^{DW1572C/+}$). * p<0.05, ** p<0.01, † p<0.001, ‡ p<0.0001. **e,** CD11b(-)CD3(-)CD19(-)CD317(high) cells are expressing interferon α, as expected for activated pDCs, as well as interleukin-6. Percentages shown indicate % of total dermal cells. n = 5 (*Fbn1*$^{+/+}$, +/+), 4 (*Fbn1*$^{D1545E/+}$, DE/+), 4 (*Fbn1*$^{DW1572C/+}$, WC/+). * p<0.05, ** p<0.01, † p<0.001, ‡ p<0.0001.

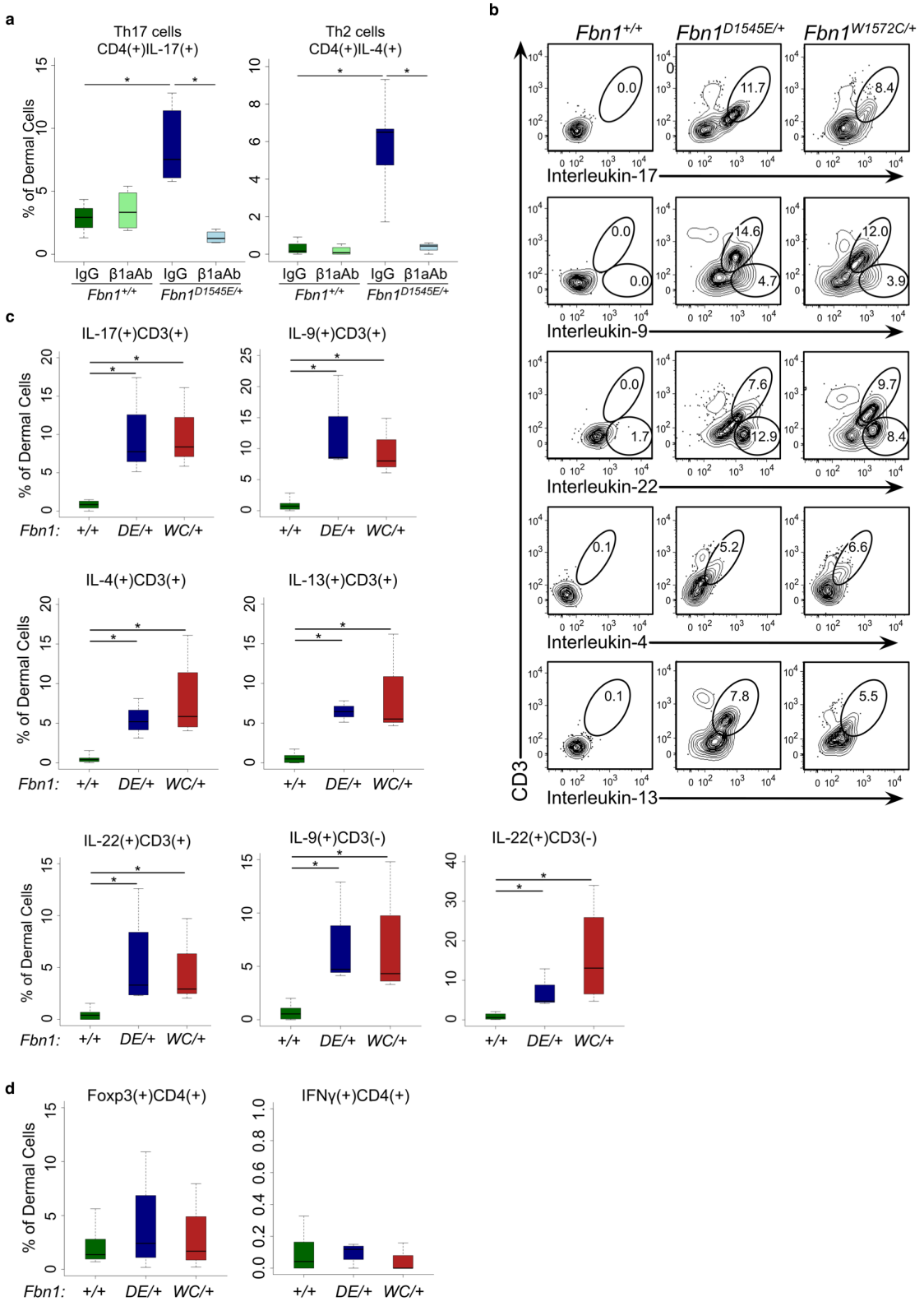

Supplementary Figure S9 | β1 antibody treatment prevents the skewing of T helper cells. a, The skewing of T helper (Th) CD4(+) lymphocytes toward IL-4(+) Th2 and IL-17(+) Th17 populations in mutant mice was prevented upon treatment with β1aAb. Isotype control-treated: n = 5 (*Fbn1*$^{+/+}$), 7 (*Fbn1*$^{D1545E/+}$); β1aAb-treated: n = 4 (*Fbn1*$^{+/+}$), 7 (*Fbn1*$^{D1545E/+}$). For panel E: n = 5 (*Fbn1*$^{+/+}$), 4 (*Fbn1*$^{D1545E/+}$), 4 (*Fbn1*$^{DW1572C/+}$). * p<0.05, ** p<0.01, † p<0.001, ‡ p<0.0001. **b,**

Representative flow cytometry plots of dermal cells positive for CD3 and interleukins 17, 9, 22, 4, and 13. **c,** Quantification by boxplot shows increases in CD3(+) cells also positive for interleukins 17, 9, 22, 4, and 13, and in CD3(-) cells also positive for interleukins-9 or interleukin-22. **d,** There were no changes in either FoxP3(+) CD4(+)T-regulatory (Treg) or IFNγ(+) CD4(+)Th1 cells in the dermis of SSS mice. All mice were male and 2 months of age. n = 5 (*Fbn1*$^{+/+}$, +/+), 4 (*Fbn1*$^{D1545E/+}$, DE/+), 4 (*Fbn1*$^{DW1572C/+}$, WC/+). * p<0.05, ** p<0.01, † p<0.001, ‡ p<0.0001.

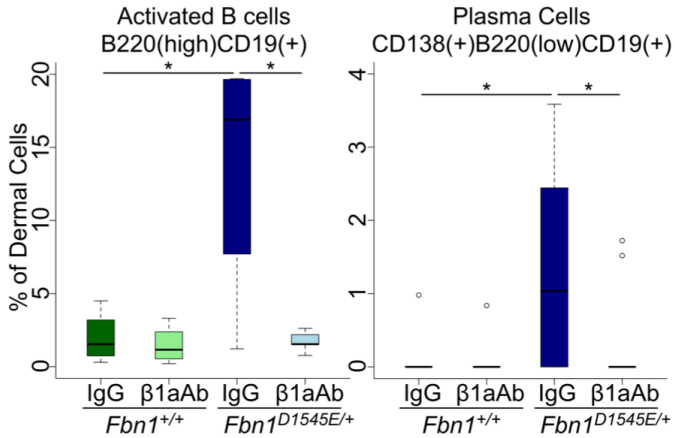

Supplementary Figure S10 | β1 antibody treatment prevents dermal accumulation of activated B cells and plasma cells. Mutant mice showed accumulation of B220(high)CD19(+) activated B cells and CD138(+)B220(low)CD19(+) plasma cells in the dermis that was prevented by treatment with β1aAb but not an isotype-matched control (IgG). Isotype control-treated: n = 5 (*Fbn1*$^{+/+}$), 7 (*Fbn1*$^{D1545E/+}$); β1aAb-treated: n = 4 (*Fbn1*$^{+/+}$), 7 (*Fbn1*$^{D1545E/+}$). For panel E: n = 5 (*Fbn1*$^{+/+}$), 4 (*Fbn1*$^{D1545E/+}$), 4 (*Fbn1*$^{DW1572C/+}$). * p<0.05, ** p<0.01, † p<0.001, ‡ p<0.0001.

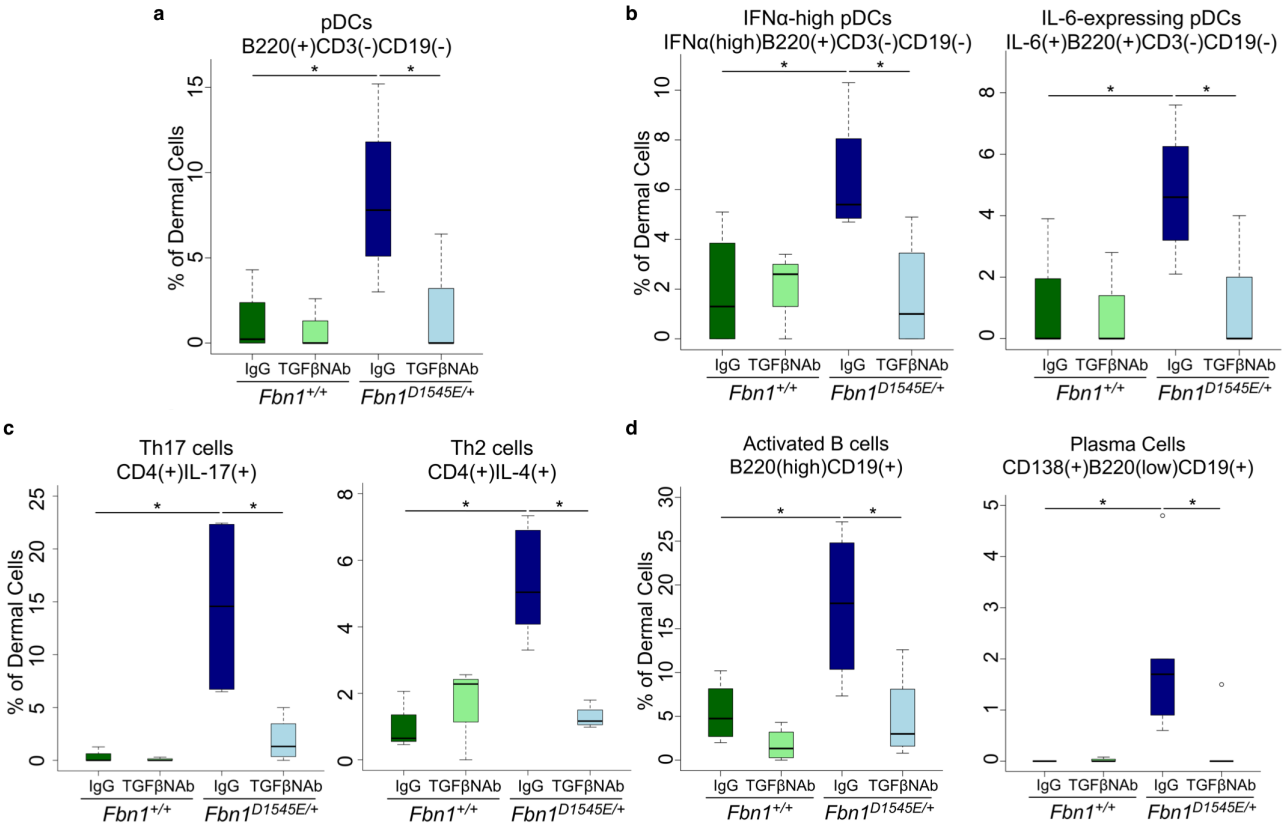

Supplementary Figure S11 | TGF-β neutralizing antibody treatment reverses dermal immune cell infiltration and activation in SSS mice. a, TGF-β neutralizing antibody (TGFβNAb) reverses accumulation of pDCs (defined by B220(+)CD3(-)CD19(-)) in the dermis of *Fbn1*$^{D1545E/+}$ mice, and **b,** the expression of both IFNα and IL-6 in these cells. Both **c,** the skewing of T helper (Th) CD4(+) lymphocytes toward IL-4(+) Th2 and IL-17(+) Th17 populations, and **d,** the accumulation of B220(high)CD19(+) activated B cells and CD138(+)B220(low)CD19(+) plasma cells in the dermis of *Fbn1*$^{D1545E/+}$ mice were reversed upon treatment with TGFβNab, but not an isotype-matched control (IgG). Isotype control-treated: n = 4 (*Fbn1*$^{+/+}$), 4 (*Fbn1*$^{D1545E/+}$). TGFβNAb-treated: n = 4 (*Fbn1*$^{+/+}$); 4 (*Fbn1*$^{D1545E/+}$). * p<0.05, ** p<0.01, † p<0.001, ‡ p<0.0001.

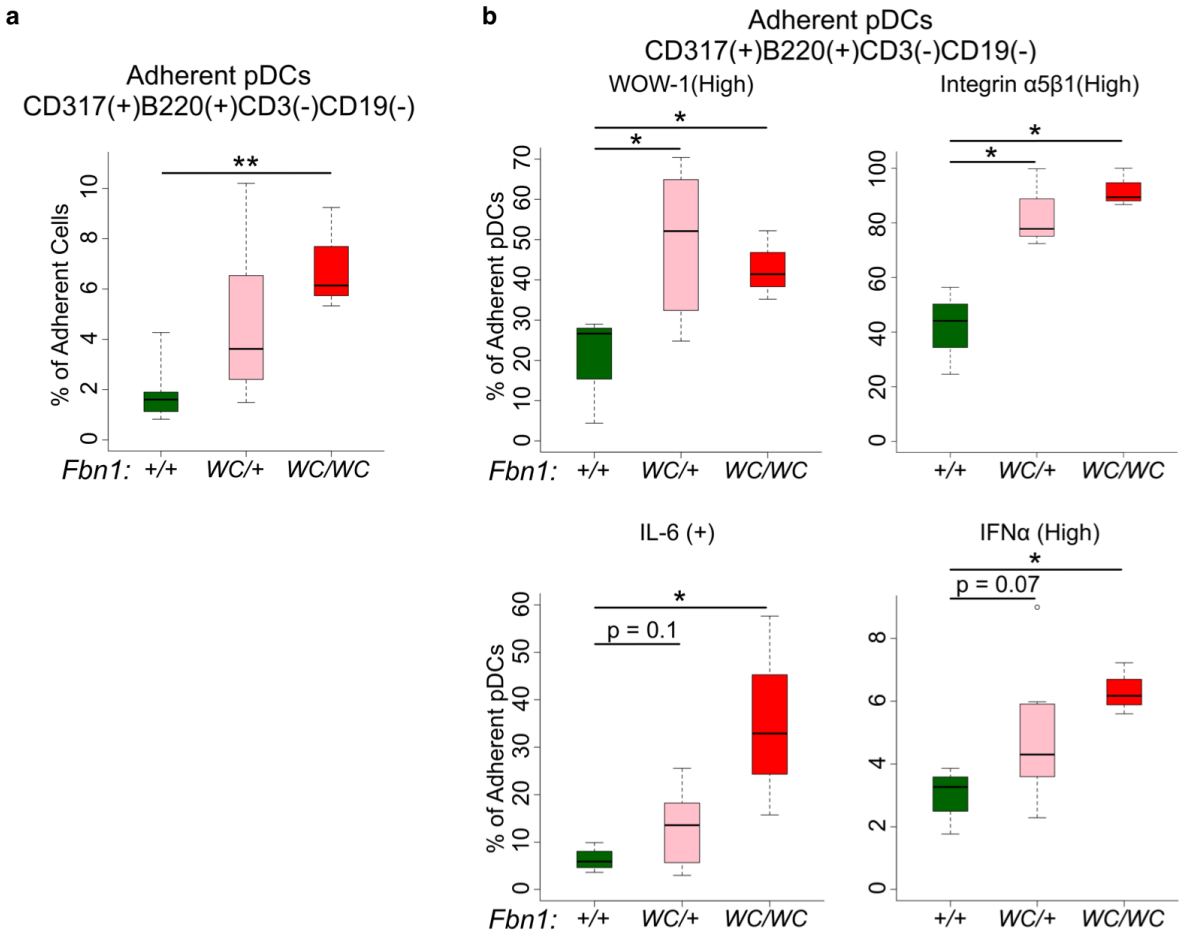

Supplementary Figure S12 | Adherence and activation of plasmacytoid dendritic cells (pDCs) *in vitro*. a, Wild-type spleen-derived pDCs show an increase in adherence to the matrix elaborated by murine embryonic fibroblasts (MEFs) derived from *Fbn1*$^{W1572C/+}$ (WC/+, n = 8) and *Fbn1*$^{W1572C/W1572C}$ (WC/WC, n = 4) SSS mice, when compared to *Fbn1*$^{+/+}$ (+/+, n = 6) mice. **b,** Among adherent pDCs, those plated on mutant MEFs show increased expression of WOW-1, integrin α5β1, IL-6, and IFNα. * p<0.05, ** p<0.01, † p<0.001, ‡ p<0.0001.

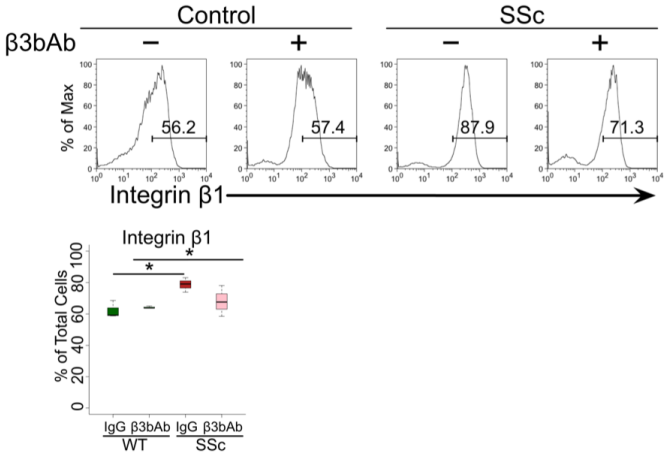

Supplementary Figure S13 | Cultured SSc dermal fibroblasts show increased total β1 integrin by flow cytometry. Treatment with β3 integrin-blocking antibody (β3bAb) did not significantly reduce cell-surface presentation of total β1 integrin. Quantifications reflect the analysis of 6 control and 5 SSc cell lines. * $p<0.05$.

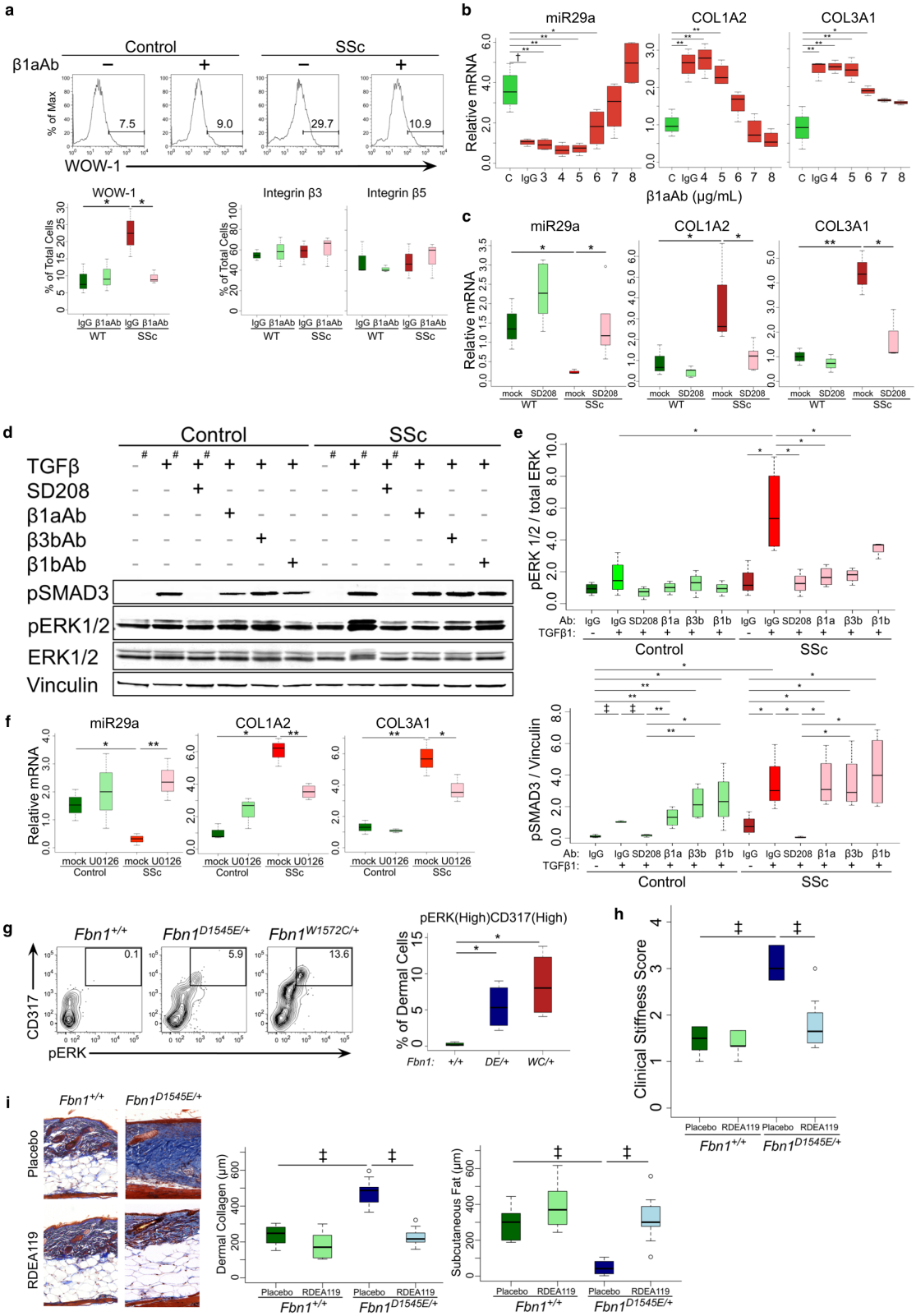

Supplementary Figure S14 | Expression and signaling abnormalities in SSc fibroblasts are attenuated by integrin-modulating antibodies. a, Cultured primary SSc fibroblasts show high surface expression of WOW-1 that was normalized by treatment with β1aAb. Representative flow cytometry histograms depict the percent of maximum (y-axis) at various fluorescent

intensities (x-axis), as described in Supplemental Methods. Quantification of the percent of positive cells is also shown. Total αvβ3 and αvβ5 were normal in SSc cells and did not change with treatment. **b,** Cultured SSc fibroblasts (red) show low expression of microRNA-29a (miR-29a) and high expression of messenger RNAs (mRNAs) derived from the genes encoding types IA2 (COL1A2) and III (COL3A1) collagens, when compared to age- and gender-matched control fibroblasts (green); each of these abnormalities was normalized upon treatment with β1aAb in a dose-dependent manner. **c,** SD208, an antagonist of the kinase activity of the type I TGFβ receptor subunit (TβRI), normalizes expression of the genes encoding type IA2 and III collagens in primary dermal fibroblasts derived from patients with SSc. Although treatment increased expression of miR-29a, this finding did not reach significance. (D, E) Control fibroblasts show phosphorylation of Smad3 (pSMAD3) in response to 5 minutes of stimulation with TGFβ1, without a change in phosphorylated extracellular regulated kinase1/2 (pERK1/2). Neither signaling cascade was attenuated by β1aAb, β3bAb or β1 integrin-blocking antibody (β1bAb). In contrast, SSc fibroblasts uniquely show ERK1/2 activation (pERK1/2) in response to TGFβ1 that was normalized after treatment with β1aAb or β3bAb but not β1bAb. Both Smad3 and ERK1/2 activation were sensitive to treatment with SD208, an antagonist of the kinase activity of the type I TGFβ receptor subunit (TβRI). **f,** U0126, an inhibitor of the mitogen-activated protein kinase/ERK kinase (MEK), increases miR-29a expression and reduces type IA2 and III collagen expression in SSc fibroblasts. Quantifications for panels A-F reflect the analysis of 6 control and 5 SSc cell lines. * $p<0.05$, ** $p<0.01$, † $p<0.001$, ‡ $p<0.0001$. **g,** Flow cytometry reveals that CD317(+) pDCs show high phosphorylation of ERK1/2 (pERK) in SSS mouse models; n = 5 (*Fbn1*$^{+/+}$), 4 (*Fbn1*$^{D1545E/+}$), 4 (*Fbn1*$^{DW1572C/+}$). (H,I) MEK inhibitor RDEA119 prevents skin stiffness, dermal collagen accumulation and loss of subcutaneous fat in *Fbn1*$^{D1545E/+}$ mice. For panels G-I, Isotype control-treated: n = 11 (*Fbn1*$^{+/+}$), 10 (*Fbn1*$^{D1545E/+}$); RDEA119-treated: n = 10 (*Fbn1*$^{+/+}$), 10 (*Fbn1*$^{D1545E/+}$). * $p<0.05$, ** $p<0.01$, † $p<0.001$, ‡ $p<0.0001$.

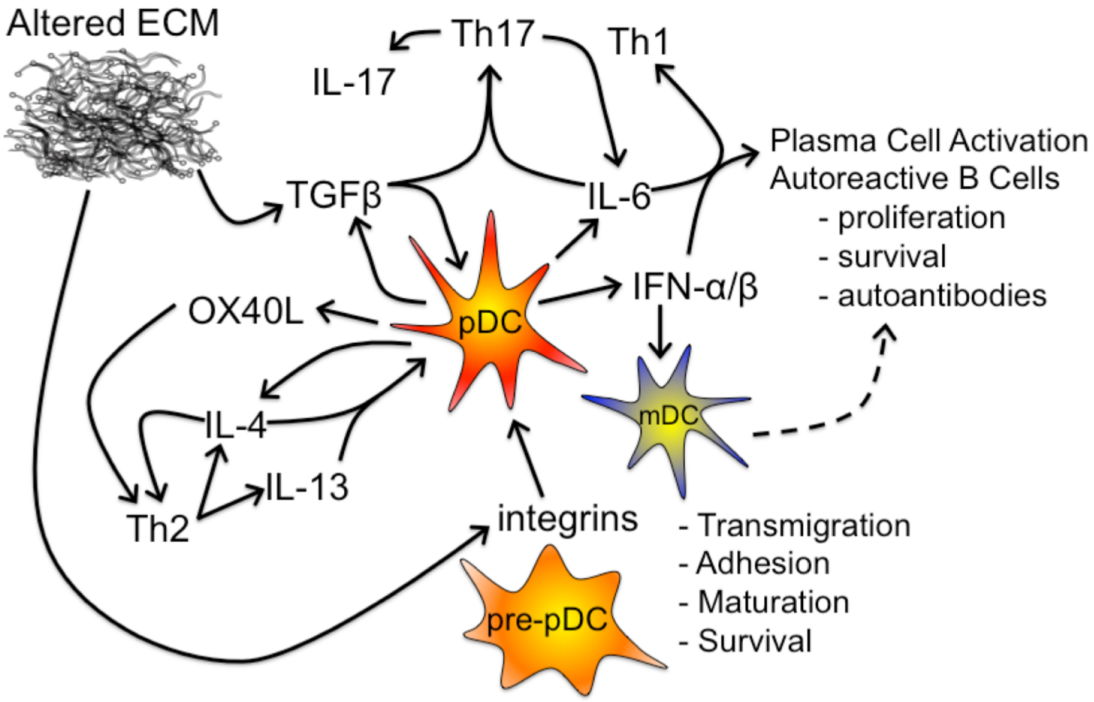

Supplementary Figure S15 | Events influencing and influenced by plasmacytoid dendritic cells (pDCs). The abnormal extracellular matrix (ECM) in SSS leads to concentration of TGFβ in the skin. TGFβ can induce expression of itself and IL-6 by pDCs; the combination of TGFβ and IL-6 leads to Th17 skewing. pDCs also secrete type I interferon (IFN-α/β), which together with IL-6 can induce Th1 polarization and the activation/maturation of plasma cells and autoreactive B cells. IFN-α/β can also induce myeloid dendritic cells (mDCs) to phagocytize cellular debris, which can indirectly contribute to autoantibody production (dashed arrow). pDCs can also contribute to Th2 polarization through secretion of OX40L or IL-4 and the Th2 cytokines IL-4 and IL-13 can influence pDC performance. The expression of integrins by pre-pDCs, perhaps in response to an altered ECM, can influence their transmigration, adhesion and/or maturation to pDCs.

a

	IgG-treated Fbn1$^{+/+}$	β1aAb-treated Fbn1$^{D1545E/+}$	Nml Range	p-value
White Blood Cells (K/μL)	3.05 ± 0.79	3.54 ± 0.52	1.8 -10.7	0.42
Neutrophils (K/μL)	0.78 ± 0.08	0.72 ± 0.16	0.1-2.4	0.62
Lymphocytes (K/μL)	2.12 ± 0.65	2.63 ± 0.57	0.9-9.3	0.36
Monocytes (K/μL)	0.12 ± 0.06	0.13 ± 0.04	0.0-0.4	0.82
Eosinophils (K/μL)	0.03 ± 0.04	0.04 ± 0.05	0.0-0.02	0.80
Basophils (K/μL)	0.01 ± 0.02	0.02 ± 0.02	0.0-0.2	0.69
Platelets (K/μL)	740 ± 190	694 ± 230	592 -2972	0.80
Red Blood Cells (M/μL)	9.55 ± 0.90	9.34 ± 0.43	6.36-9.42	0.73
Hematocrit (%)	45.67 ± 0.78	47.40 ± 2.42	35.1-45.4	0.55

b

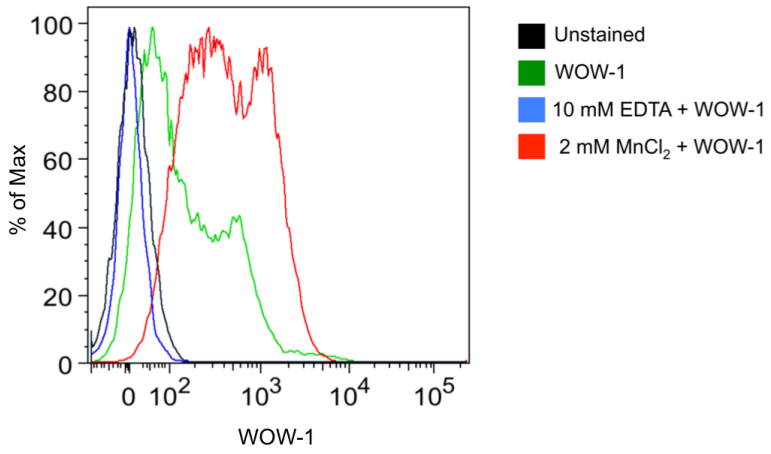

Supplementary Figure S16 | a, There were no differences in final blood cell counts between isotype control- and β1aAb-treated animals. n = 3 for each experimental group. Nml Range = the normal values reported by the Comparative Pathology Laboratory at Johns Hopkins University School of Medicine. K/ μL = thousands per cubic microliter of blood. M/ μL = millions per cubic microliter of blood. **b,** Specificity of the WOW-1 antibody was assessed in control fibroblasts by flow cytometry. As expected, chelation of calcium with 10 mM Ethylenediaminetetraacetic acid (EDTA) – an event known to prevent the active conformation of αvβ3 – reduced immunoreactivity, while treatment with 2 mM $MnCl_2$ – known to activate αvβ3 – increased immunoreactivity.